Exploration of the Four-Dimensional-Conformational Potential Energy Hypersurface of *N*-Acetyl-L-aspartic Acid *N*′-Methylamide with Its Internally Hydrogen Bonded Side-Chain Orientation

Joseph C. P. Koo,[†] Gregory A. Chass,[†,‡] Andras Perczel,[§] Ödon Farkas,[§] Ladislaus L. Torday,[||] Andras Varro,[||] Julius Gy. Papp,[||,⊥] and Imre G. Csizmadia*[,†]

Department of Chemistry, University of Toronto, Toronto, Ontario, Canada, M5S 3H6, Velocet R & D, 210 Dundas Street West, Suite 810, Toronto, Ontario, Canada M5G 2E8, Department of Organic Chemistry, Eotvos University, H-1117, Budapest, Hungary, Department of Pharmacology and Pharmacotherapy, Szeged University, Dóm tér 12, H-6701, Szeged, Hungary, and Division of Cardiovascular Pharmacology, Hungarian Academy of Sciences and Szeged University, Dóm tér 12, H-6701, Szeged, Hungary

Received: December 13, 2001; In Final Form: March 28, 2002

Side-chain conformational potential energy hypersurfaces have been generated and analyzed for each of the nine possible backbone conformers of *N*-acetyl-L-aspartic acid-*N*′ methylamide. A total of 37 out of the 81 possible conformers were found and optimized at the B3LYP/6-31G(d) level of theory. The relative energies as well as the stabilization exerted by the side-chain on the backbone have been calculated, at this level of theory, for the 37 optimized conformers. Various backbone-backbone (N−H···O═C) and backbone-side-chain (N−H···O═C; N−H···OH) hydrogen bonds were analyzed. The appearance of the notoriously absent α_L backbone conformer was attributed to such a backbone-side-chain (BB−SC) hydrogen bonds as well as a very unusual backbone-backbone (BB−BB) hydrogen bond.

Introduction

Stereo Chemical Background. In recent years, many studies have been performed on the potential energy hypersurfaces (PEHS) containing various amino acid residues.[1] The ultimate hope of such research is to be able to predict the stable conformations of oligo- and polypeptides[2] composed of naturally occurring amino acids. Most amino acids, with the exception of glycine (and to some degree proline), may be regarded as a side-chain substituted (**I**) alanine (**II**). Conformation of amino acid residues may be characterized, at least partially, by four torsional angles: ϕ, ψ, χ_1, and χ_2. This is also the case for the aspartyl residue in **III**. This leads to a PEHS(1) of four independent variables (4D):

$$E = \mathrm{E}(\phi, \psi, \chi_1, \chi_2) \tag{1}$$

If the variables are separated to side-chain dihedral angles (χ_1, χ_2) and backbone torsional angles (ϕ, ψ), then the 4D PEHS can be partitioned to a pair of 2D-potential energy surfaces (PESs)(2,3):

$$E = (\chi_1, \chi_2) \tag{2}$$

$$E = (\phi, \psi) \tag{3}$$

The latter PES(3) is frequently referred to as the "Ramachandran Map" (Figure 1). For example, using the alanyl residue, extensive computation studies have been performed on oligopeptides.[3−7] In addition, various single amino acid-diamides, including asparagines,[8] glycine,[9,10] valine,[11] phenylalanine,[12−14] serine,[15−17] glutamic acid,[18,19] leucine,[20] cysteine,[21] selenocysteine,[22] and proline,[23] have been subjected to detailed *ab initio* computations.

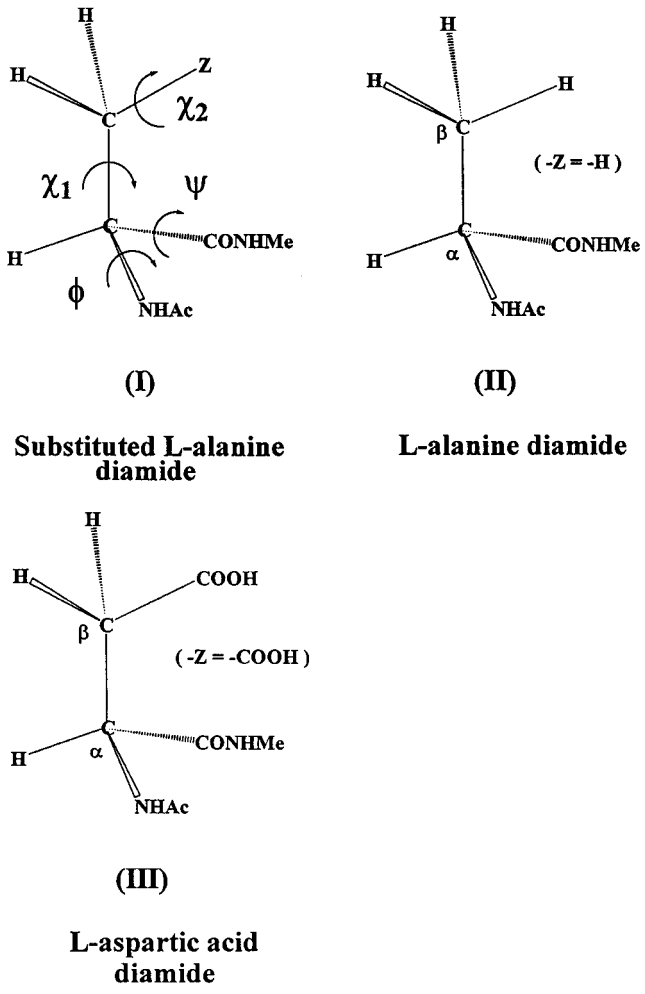

* Corresponding author. E-mail: icsizmad@alchemy.chem.utoronto.ca.
† Department of Chemistry.
‡ Velocet R & D.
§ Department of Organic Chemistry.
|| Department of Pharmacology and Pharmacotherapy.
⊥ Division of Cardiovascular Pharmacology.

10.1021/jp014514b CCC: $22.00
Published on Web 07/10/2002

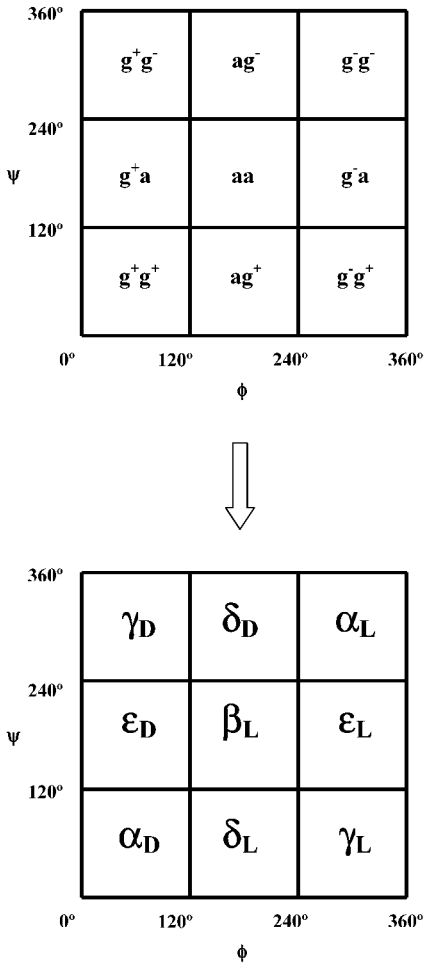

Figure 1. Topology of a Ramachandran Potential Energy Surface (PEHS), E = E (ϕ, ψ) of an amino acid residue in a peptide. (Top) Conformers are designated by IUPAC conventions. (Bottom) Conformers are designated by traditional conventions.

In this particular research, computational calculations were performed on *N*-acetyl-L-aspartic acid *N*′-methylamide (where Z = −COOH, in **III**) in order to gain a better understanding in its role in a peptide chain. *N*-Acetyl-L-aspartic acid *N*′-methylamide, shown in Figure 2, has in both of its N- and C-termini a methyl group. The methyl groups were designed to mimic the α-carbon of the next amino acid in a tripeptide unit of a polypeptide chain. In an earlier study, Salpietro et al.[24] reported the side-chain conformational potential energy surface, $E = E(\chi_1, \chi_2)$, of *N*-formyl-L-aspartic acidamide only in its γ_L backbone conformation. *N*-Formyl-L-aspartic acidamide, in contrast to *N*-acetyl-L-aspartic acid *N*′-methylamide, has H atoms instead of methyl groups at its N- and C-termini. In that exploratory study,[24] it was found that the stability of certain side-chain conformers for *N*-formyl-L-aspartic acidamide in its γ_L backbone conformation was due to internal hydrogen bonding. Thus, we aim to investigate whether internal side-chain-backbone hydrogen bonding, in addition to backbone-backbone hydrogen bonding, is truly the underlying cause in stabilizing the various conformers of the aspartic acid residue. The backbone geometry of *N*-acetyl-L-aspartic acid *N*′-methylamide is expected to be similar to an alanyl residue (**II**). However, in this case, the −COOH group is replacing one of the H atoms on the side-chain methyl group of alanine (**III**). Alanine is the simplest chiral amino acid whose backbone can be found in most other peptide residues.

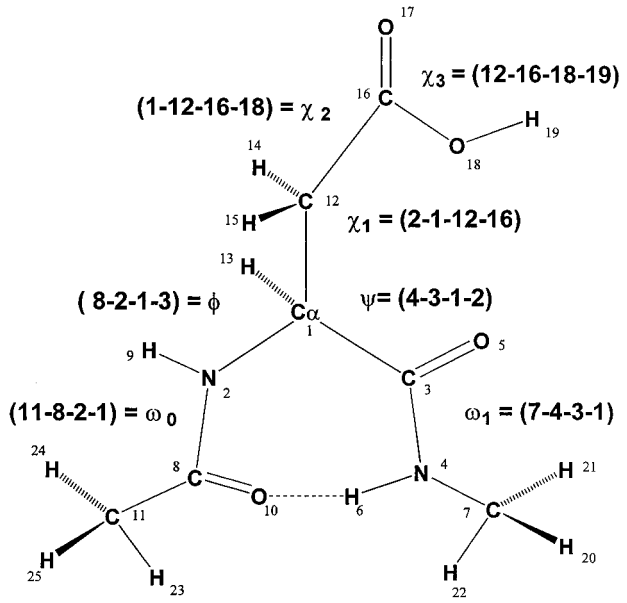

Figure 2. Atomic Numbering and definition of torsional angles for *N*-acetyl-L-aspartic acid *N*′-methylamide.

Since earlier computational studies of the alanyl residue[25−30] could not find stable conformers in the α_L and ϵ_L backbone, it is expected that no stable conformers in these backbone could be found for *N*-acetyl-L-aspartic acid *N*′-methylamide. In the present study, backbone (ϕ, ψ) and side-chain (χ_1, χ_2) variations of *N*-acetyl-L-aspartic acid *N*′-methylamide would lead to a 4D-Ramachandran potential energy hypersurface (PEHS): $E = E(\phi, \psi, \chi_1, \chi_2)$. As a result, $3^4 = 81$ geometries need to be computationally optimized on a 4D-Ramachandran PEHS, shown in Figure 3. Moreover, in principle, the backbone conformation could lead up to $3^2 = 9$ structures (γ_L, β_L, δ_L, α_L, ϵ_L, γ_D, δ_D, α_D, and ϵ_D) on the 2D-Ramachandran map, coupled with $3^2 = 9$ side-chain orientations for each of the nine possible backbone conformation.

Biological Background. *Ab initio* study on *N*-acetyl-L-aspartic acid *N*′-methylamide will deem beneficial to help gain better understanding on the many active conformations of any oligopeptide containing an aspartic acid residue. One prominent example is Arg-Gly-Asp (RGD), which is a common tripeptide sequence shared by many adhesive proteins, such as collagens, fibronectin, and fibrinogen (Figure 4).[31] Studies on the RGD tripeptide of these adhesive proteins allow better understanding on important biological processes, such as cell adhesion and a virus' recognition of host receptor that leads to its attachment. In turn, studies in protein adhesion have led to advances in gene therapy; for instance, the adenovirus vector has shown promising results in gene delivery.[32−36]

Having recognized the relevance of studying the *N*-acetyl-L-aspartic acid *N*′-methylamide in its relation to the further RGD studies, the aspartic acid residue itself is also a molecule of great interest. For example, mutations in the aspartate regions on the human immunodeficiency virus-1 (HIV-1) chemokine receptor CXCR4 would greatly reduce the receptor's function in HIV-1 host entry.[37] Other RGD-related biological implications include the induction of apoptosis[38] as well as antitumor activity against human lung cancer.[39]

Studies in the aspartic acid residue itself is important in many fields, including quantitative measurements of cerebral injury for stroke patients,[40] protein decomposition,[41] antibody selectivity,[42] study in Alzeimer's Disease,[43] lipase activities,[44] probing

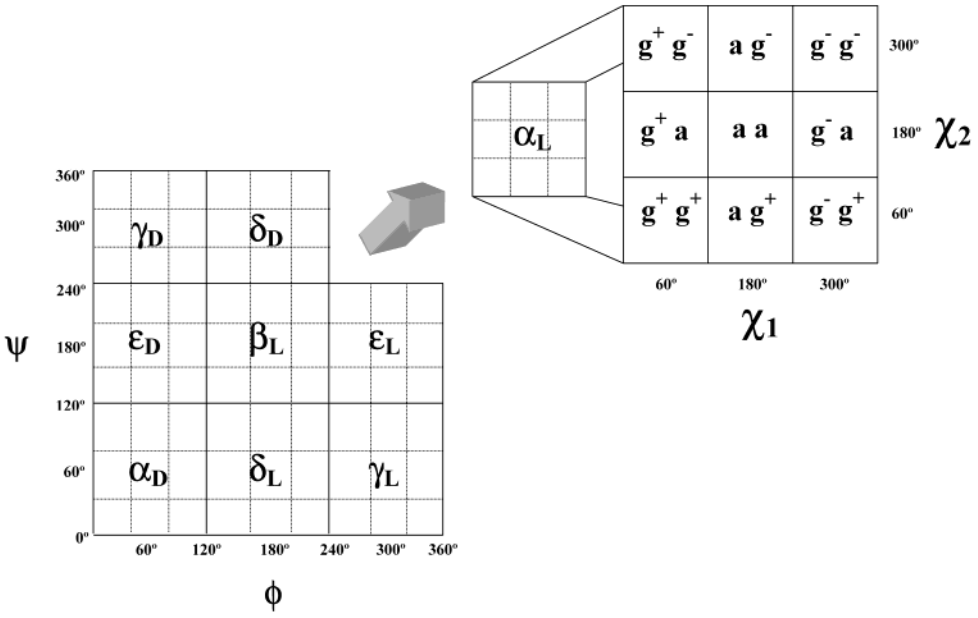

Figure 3. A schematic representation of the 4D Ramachandran PEHS $E = E(\phi, \psi, \chi_1, \chi_2)$. Each of the nine backbone conformations (γ_L, β_L, δ_L, α_L, ϵ_L, γ_D, δ_D, α_D, and ϵ_D) have nine side-chain conformation as shown by the α_L conformation.

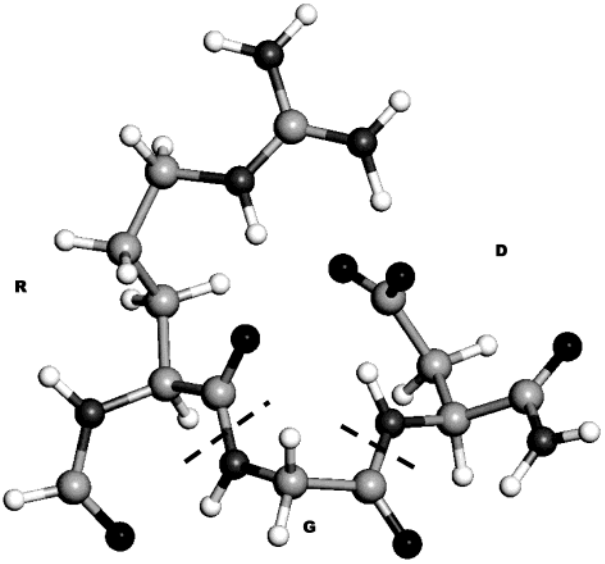

Figure 4. An Arg-Gly-Asp (RGD) conformer obtained by preliminary optimization.[31]

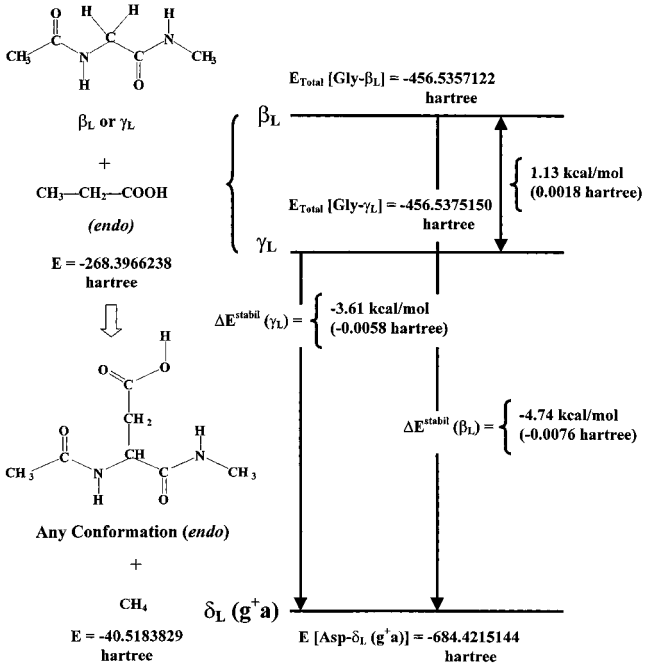

Figure 5. Definition of stabilization energies of *N*-acetyl glycine *N*′ methylamide with respect to the γ_L or β_L conformers of *N*-acetyl-L-aspartic acid *N*′-methylamide. This is a schematic illustration and the diagram is not to scale.

of the binding sites for HIV-1 protease,[45] immunological antiproliferative studies,[46] and enzyme kinematics in bacteria.[47]

In a recent study it was found that a stable conformation of RGD, which enhances oral bioavailability, greatly affects its molecular geometry and hydrogen bonding ability.[48] This report reaffirms the importance of understanding the conformation of RGD. Hence, investigating the individual components of the RGD tripeptide using *ab initio* methods may deem essential, especially when hydrogen bonding and molecular geometry are affected.

In this paper, we wish to report all possible backbone and side-chain conformers that may exist in *N*-acetyl-L-aspartic acid *N*′-methylamide, with an *endo* −OH orientation in the side-chain −COOH, which was shown to be the most stable form by the previous exploratory study.[24]

Computational Methods. GAUSSIAN 94[49] and GAUSSIAN 98[50] were used to carry out *ab initio* calculations on all possible side-chain conformers of the nine backbone conformations (γ_L, β_L, δ_L, α_L, ϵ_L, γ_D, δ_D, α_D, and ϵ_D) for *N*-acetyl-L-aspartic acid *N*′-methylamide to determine its minima on the conformational potential energy hyper surface (PEHS) as illustrated in Figure 3. The initial γ_L backbone and side-chain geometries were taken from the previously published *N*-formyl-L-aspartic acidamide results.[24] Here, the geometric characteristics of the side-chain can be related to CH_3-CH_2-COOH. Given these parameters, partially relaxed PEHS double-scan calculations were first performed for *N*-acetyl-L-aspartic acid *N*′-methylamide under normal conditions where (FOPT = **Z**-MATRIX). Hence, grid

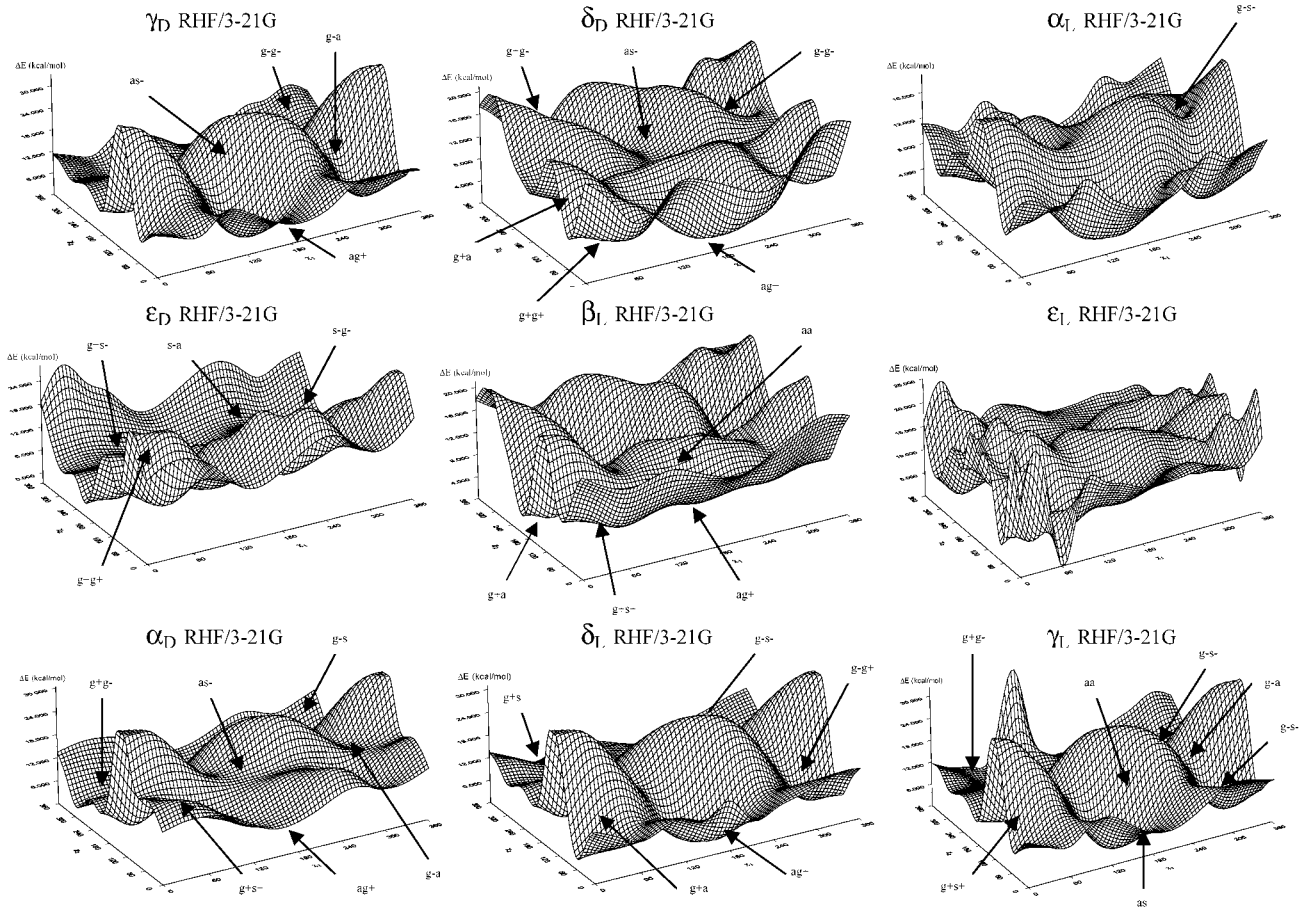

Figure 6. Landscape representation of the nine side-chain conformational PEHSs, $E = E(\chi_1, \chi_2)$ associated with each one of the nine backbone conformations. Torsional angles χ_1 and χ_2 are given in degrees.

points for these scan calculations all had gradients of less than 4.5×10^{-4} au. In these double-scan calculations, the amino acid backbone was fixed to its typical conformations (γ_L, β_L, δ_L, α_L, ϵ_L, γ_D, δ_D, α_D, and ϵ_D) by specifying and restricting the ϕ and ψ torsional angles while the two side-chain variables, χ_1 and χ_2, were rotated with 30.0° increments, producing a total of $12 \times 12 = 144$ points. These double-scan results serve as preliminary estimates of where possible side-chain conformers for each backbone may be found. Subsequently, tight geometry optimizations were performed at the RHF/6-31G(d) and B3LYP/6-31G(d) levels of theory using Berny optimization (FOPT = TIGHT, **Z**-MATRIX), which at termination produced a gradient of less than 1.5×10^{-5} au for all critical points. Only the B3LYP/6-31G(d) results are reported in the present paper.

With the aid of CH_3-CH_2-COOH, energy values of the stabilization exerted by the side-chain on the backbone were calculated using the following isodesmic reactions with respect to the $\gamma_L(4)$ and $\beta_L(5)$ backbones of the glycine residue quoting only the B3LYP/6-31G(d) energy values:

where CH_3-R stands for CH_3-CH_2-COOH and $CH_3CO-(NH-CHR-CO)-NHCH_3$ stands for *N*-acetyl-L-aspartic acid *N*′-methylamide, respectively. An example of the stabilization energy calculation is illustrated on Figure 5.

Results and Discussion

Initially the side-chain PESs, $E = E(\chi_1, \chi_2)$ were generated for each one of the nine backbone conformations (γ_L, β_L δ_L, α_L, γ_D, δ_D, α_D, ϵ_D). The nine side-chain PESs, shown in landscape representation Figure 6 and contour representation Figure 7, exhibited numerous minima. When these apparent minima were optimized only some of them turned out to be true minima. Such discrepancy may well be expected since the torsional angles ϕ and ψ were frozen. Furthermore, it has to be recognized that in a double scan such as $E = E(\chi_1, \chi_2)$, grid points are optimized at fixed $\chi_1$and χ_2 values. Consequently, these semirigid optimizations do not precisely correspond to optimized structures. Thus, any minimum appearing on a surface

$$\underset{\gamma_L}{CH_3-CO-(NH-CH_2-CO)-NHCH_3} + CH_3-R \rightarrow \underset{\text{any conformation}}{CH_3CO-(NH-CHR-CO)-NHCH_3} + CH_4 + \Delta E^{stab}(\gamma_L) \quad (4)$$

$$\underset{\text{hartree}}{-456.5375150} \qquad \underset{\text{hartree}}{-268.3966238} \qquad \underset{\text{hartree}}{-40.5183829}$$

$$\underset{\beta_L}{CH_3-CO-(NH-CH_2-CO)-NHCH_3} + CH_3-R \rightarrow \underset{\text{any conformation}}{CH_3CO-(NH-CHR-CO)-NHCH_3} + CH_4 + \Delta E^{stab}(\beta_L) \quad (5)$$

$$\underset{\text{hartree}}{-456.5357122} \qquad \underset{\text{hartree}}{-268.3966238} \qquad \underset{\text{hartree}}{-40.5183829}$$

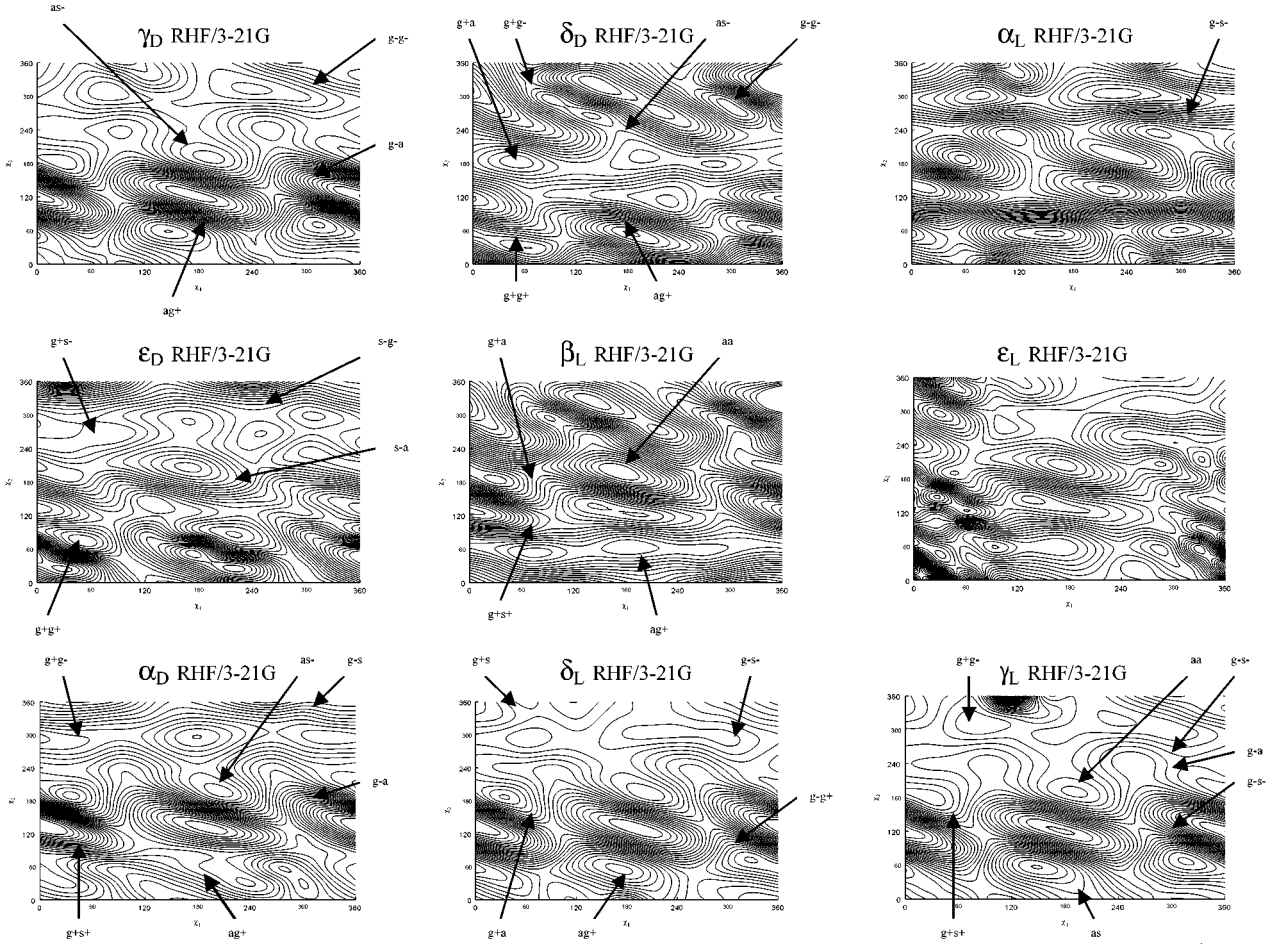

Figure 7. Contour representation of the nine side-chain conformational PEHSs, $E = E(\chi_1, \chi_2)$ associated with each one of the nine backbone conformations. Torsional angles χ_1 and χ_2 are given in degrees.

TABLE 1: A Summary of All Conformers "Converged" or "Not Found" for *N*-Acetyl-L-aspartic Acid *N*′-Methylamide in Its *endo* Form: All Its Stable Backbone (γ_L, β_L, δ_L, α_L, ϵ_L, γ_D, δ_D, α_D, and ϵ_D) Conformations Computed at the B3LYP/6-31G(d) Level of Theory

	initial		final				initial		final				initial		final		
BB	χ_1	χ_2	χ_1	χ_2	convergence	BB	χ_1	χ_2	χ_1	χ_2	convergence	BB	χ_1	χ_2	χ_1	χ_2	convergence
γ_L	g^+	g^+			not found	α_L	g^+	g^+			not found	δ_D	g^+	g^+	g^+	g^+	converged
γ_L	g^+	a	g^+	s^+	converged	α_L	g^+	a			not found	δ_D	g^+	a	g^+	a	converged
γ_L	g^+	g^-	g^+	g^-	converged	α_L	g^+	g^-			not found	δ_D	g^+	g^-	g^+	g^-	converged
γ_L	a	g^+	a	s	converged	α_L	a	g^+			not found	δ_D	a	g^+	a	g^+	converged
γ_L	a	a	a	a	converged	α_L	a	a			not found	δ_D	a	a	a	s^-	converged
γ_L	a	g^-	−	−	not found	α_L	a	g^-			not found	δ_D	a	g^-			not found
γ_L	g^-	g^+	g^-	s^+	converged	α_L	g^-	g^+			not found	δ_D	g^-	g^+			not found
γ_L	g^-	a	g^-	a	converged	α_L	g^-	a	g^-	s^-	converged	δ_D	g^-	a			not found
γ_L	g^-	g^-	g^-	s^-	converged	α_L	g^-	g^-			not found	δ_D	g^-	g^-	g^-	g^-	converged
β_L	g^+	g^+	g^+	s^+	converged	ϵ_L	g^+	g^+			not found	α_D	g^+	g^+	g^+	s^+	converged
β_L	g^+	a	g^+	a	converged	ϵ_L	g^+	a			not found	α_D	g^+	a			not found
β_L	g^+	g^-	−	−	not found	ϵ_L	g^+	g^-			not found	α_D	g^+	g^-	g^+	g^-	converged
β_L	a	g^+	a	g^+	converged	ϵ_L	a	g^+			not found	α_D	a	g^+	a	g^+	converged
β_L	a	a	a	a	converged	ϵ_L	a	a			not found	α_D	a	a	a	s^-	converged
β_L	a	g^-			not found	ϵ_L	a	g^-			not found	α_D	a	g^-	−	−	not found
β_L	g^-	g^+			not found	ϵ_L	g^-	g^+			not found	α_D	g^-	g^+	−	−	not found
β_L	g^-	a			not found	ϵ_L	g^-	a			not found	α_D	g^-	a	g^-	a	converged
β_L	g^-	g^-			not found	ϵ_L	g^-	g^-			not found	α_D	g^-	g^-	g^-	s	converged
δ_L	g^+	g^+			not found	γ_D	g^+	g^+			not found	ϵ_D	g^+	g^+	g^+	g^+	converged
δ_L	g^+	a	g^+	a	converged	γ_D	g^+	a			not found	ϵ_D	g^+	a			not found
δ_L	g^+	g^-	g^+	s	converged	γ_D	g^+	g^-			not found	ϵ_D	g^+	g^-	g^+	s^-	converged
δ_L	a	g^+	a	g^+	converged	γ_D	a	g^+	a	g^+	converged	ϵ_D	a	g^+	−	−	not found
δ_L	a	a			not found	γ_D	a	a	a	s^-	converged	ϵ_D	a	a	s^-	a	converged
δ_L	a	g^-			not found	γ_D	a	g^-			not found	ϵ_D	a	g^-	s^-	g^-	converged
δ_L	g^-	g^+	g^-	g^+	converged	γ_D	g^-	g^+			not found	ϵ_D	g^-	g^+			not found
δ_L	g^-	a			not found	γ_D	g^-	a	g^-	a	converged	ϵ_D	g^-	a			not found
δ_L	g^-	g^-	g^-	s^-	converged	γ_D	g^-	g^-	g^-	g^-	converged	ϵ_D	g^-	g^-			not found

may not be a minimum on the hypersurface. Sometimes, such "false" minima may represent higher order critical points such as transition structures. Also, a minimum appearing on a surface may be shifted somewhat to a regional neighbor. Table 1 summarizes all the minima which were "found" and those which were "not found" during the optimization process. The position

TABLE 2: Optimized Conformers of *N*-Acetyl-L-aspartic acid *N*′-Methylamide in Its *endo* Form for All Its Stable Backbone (γ_L, β_L, δ_L, α_L, γ_D, δ_D, α_D, and ϵ_D) Conformation Computed at the B3LYP/6-31G(d) Level of Theory[a]

final conformation BB [$\chi_1\chi_2$]	optimized parameters									
	ϕ	ψ	ω_0	ω_1	χ_1	χ_2	E_{min} (hartree)	ΔE (kcal/mol)	$\Delta E^{stability}$ (kcal) γL	$\Delta E^{stability}$ (kcal) βL
					γ_L Backbone Conformation					
γ_L [g^+s^+]	−82.63	69.39	−179.63	−176.47	58.85	144.19	−684.4260542	0.000	−6.4623	−7.5936
γ_L [g^+g^-]	−83.22	70.88	−179.64	−176.59	67.76	−41.53	−684.4210847	3.118	−3.3439	−4.4751
γ_L [as]	−83.13	69.16	−178.12	−177.73	−176.54	27.91	−684.4178720	5.134	−1.3279	−2.4591
γ_L [aa]	−82.80	71.63	−179.13	−177.93	−169.19	−163.60	−684.4199177	3.851	−2.6116	−3.7428
γ_L [g^-s^+]	−83.30	71.37	−173.51	−176.48	−55.28	90.31	−684.4190950	4.367	−2.0953	−3.2266
γ_L [g^-a]	−84.30	66.13	−173.78	−177.94	−72.14	157.14	−684.4189046	4.486	−1.9758	−3.1071
γ_L [g^-s^-]	−83.95	72.82	−170.48	−175.81	−45.07	−119.39	−684.4217674	2.690	−3.7723	−4.9035
					β_L Backbone Conformation					
β_L [g^+s^+]	−170.22	150.84	−169.30	175.92	58.82	107.24	−684.4154168	6.675	0.2128	−0.9185
β_L [g^+a][b,c]	−157.77	−177.22	173.48	−179.57	66.22	−171.49	−684.4153786	6.699	0.2368	−0.8945
β_L [ag^+]	−164.40	162.84	177.73	177.71	−173.28	32.25	−684.4184974	4.742	−1.7203	−2.8516
β_L [aa]	−163.51	167.73	175.07	178.61	−161.48	173.27	−684.4240236	1.274	−5.1881	−6.3193
					δ_L Backbone Conformation					
δ_L [g^+a][b,c]	−130.74	30.06	−170.27	177.91	60.44	162.32	−684.4215144	2.849	−3.6135	−4.7448
δ_L [g^+s]	−130.53	32.86	−170.39	176.65	69.12	−26.01	−684.4164380	6.034	−0.4280	−1.5593
δ_L [ag^+]	−135.53	34.83	−170.11	175.22	−172.91	37.96	−684.4130412	8.166	1.7035	0.5722
δ_L [g^-g^+]	−135.08	25.11	−164.18	174.86	−67.72	82.47	−684.4133097	7.997	1.5350	0.4037
δ_L [g^-s^-]	−133.61	22.39	−161.57	175.51	−56.89	−98.79	−684.4155795	6.573	0.1107	−1.0206
					α_L Backbone Conformation					
α_L [g^-s^-][b,c]	−81.20	−13.35	−164.10	176.83	−55.35	−119.10	−684.4153827	6.696	0.2342	−0.8971
					γ_D Backbone Conformation					
γ_D [ag^+]	73.01	−53.01	175.99	−176.30	−170.77	65.87	−684.4128945	8.258	1.7956	0.6643
γ_D [as^-][b,c]	74.54	−65.87	178.99	177.75	−155.29	−145.77	−684.4128963	8.257	1.7944	0.6632
γ_D [g^-a]	73.63	−49.71	168.25	−178.12	−64.89	179.52	−684.4181554	4.957	−1.5057	−2.6370
γ_D [g^-g^-]	72.81	−53.52	172.24	−178.73	−59.41	−37.44	−684.4146876	7.133	0.6704	−0.4609
					δ_D Backbone Conformation					
δ_D [g^+g^+][b,c]	−155.89	−38.80	171.16	−175.78	43.03	44.58	−684.4069299	12.001	5.5384	4.4071
δ_D [g^+a][b,c]	−156.90	−48.59	174.77	−176.77	54.07	−168.35	−684.4146306	7.168	0.7061	−0.4251
δ_D [g^+g^-]	−164.26	−45.65	176.01	−175.35	67.67	−35.23	−684.4075771	11.595	5.1323	4.0010
δ_D [ag^+]	−169.53	−39.89	168.72	−171.72	178.57	65.29	−684.4067348	12.123	5.6608	4.5296
δ_D [as^-]	−173.40	−36.11	167.19	−172.40	−172.30	−117.79	−684.4058219	12.696	6.2337	5.1024
δ_D [g^-g^-][b,c]	−144.09	−61.07	178.05	−176.94	−61.73	−79.40	−684.4052097	13.080	6.6178	5.4866
					α_D Backbone Conformation					
α_D [g^+s^+]	58.20	35.63	161.69	−175.78	42.53	102.03	−684.4070563	11.921	5.4591	4.3278
α_D [g^+g^-]	59.50	29.35	164.08	−176.20	55.10	−81.81	−684.4040903	13.783	7.3203	6.1890
α_D [ag^+]	65.49	31.81	168.69	−176.91	−167.04	37.82	−684.4097827	10.211	3.7482	2.6170
α_D [as^-]	66.30	32.61	169.86	−177.78	−157.47	−149.78	−684.4122840	8.641	2.1787	1.0474
α_D [g^-a]	66.01	30.43	164.61	−177.19	−64.43	−176.83	−684.4166005	5.932	−0.5300	−1.6613
α_D [g^-s]	66.36	28.71	166.07	−177.25	−63.19	−18.36	−684.4119363	8.859	2.3968	1.2656
					ϵ_D Backbone Conformation					
ϵ_D [g^+g^+]	53.92	−123.45	−176.20	177.24	51.08	89.57	−684.4079873	11.337	4.8749	3.7436
ϵ_D [g^+s^-]	57.16	−134.18	−164.86	179.14	69.41	−103.68	−684.4113997	9.196	2.7336	1.6023
ϵ_D [s^-a]	66.93	−178.82	−158.02	−175.88	−149.86	160.48	−684.4142905	7.382	0.9196	−0.2117
ϵ_D [s^-g^-]	64.41	−167.41	−160.60	−175.48	−135.38	−50.94	−684.4076898	11.524	5.0616	3.9303

[a] Shown here are the optimized torsional angles, computed energy values, relative energies, and stabilization energies. [b] After 200 iterations under B3LYP/6-31G(d) at (TIGHT, Z-MATRIX), the force has converged, but the displacement did not converge completely. [c] This result was obtained from an optimization fully converged under regular B3LYP/6-31G(d) at (Z-MATRIX).

of the minima which were located successfully (ie. "converged") during the optimization process are also shown by arrows in Figures 6 and 7. Table 2 summarizes the optimized dihedral angles and energies of 37 optimized conformers out of grand total of 81 expected structures.

Table 2 reveals that, along χ_2, when the planar COOH moiety was rotated against the tetrahedral β-carbon, sometimes there existed a noticeable shift in the torsional angle away from the typical g^+ value (60°) or from the typical g^- value (−60°) toward the anti orientation (+180° or −180°, respectively). Such values that fell within the range of +90° and +150° (i.e., +120° ± 30°) were labeled as syn^+ (or s^+) indicating that the OH oxygen of the carboxyl moiety was in *syn* orientation with respect to the proton at about +120°. Similarly, values that fell within the range of −90° and −150° (i.e. −120° ± 30°) were labeled as syn^- (or s^-) indicating that the OH oxygen of the carboxyl moiety was in syn orientation with the proton at about −120°. Figure 8 illustrates the various hydrogen bonds that may exist in the *endo* form of *N*-acetyl-L-aspartic acid *N*′-methylamide. The corresponding distances for these hydrogen bond interactions are tabulated in Table 3. As shown in Figure 8, there exists one side-chain-side-chain (SC/SC) hydrogen bond

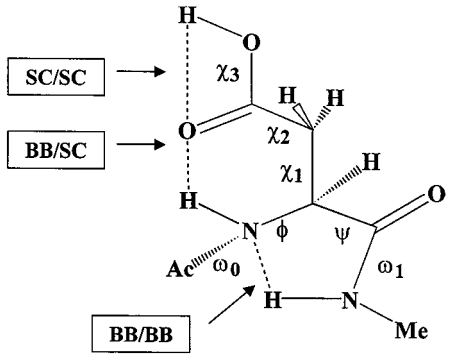

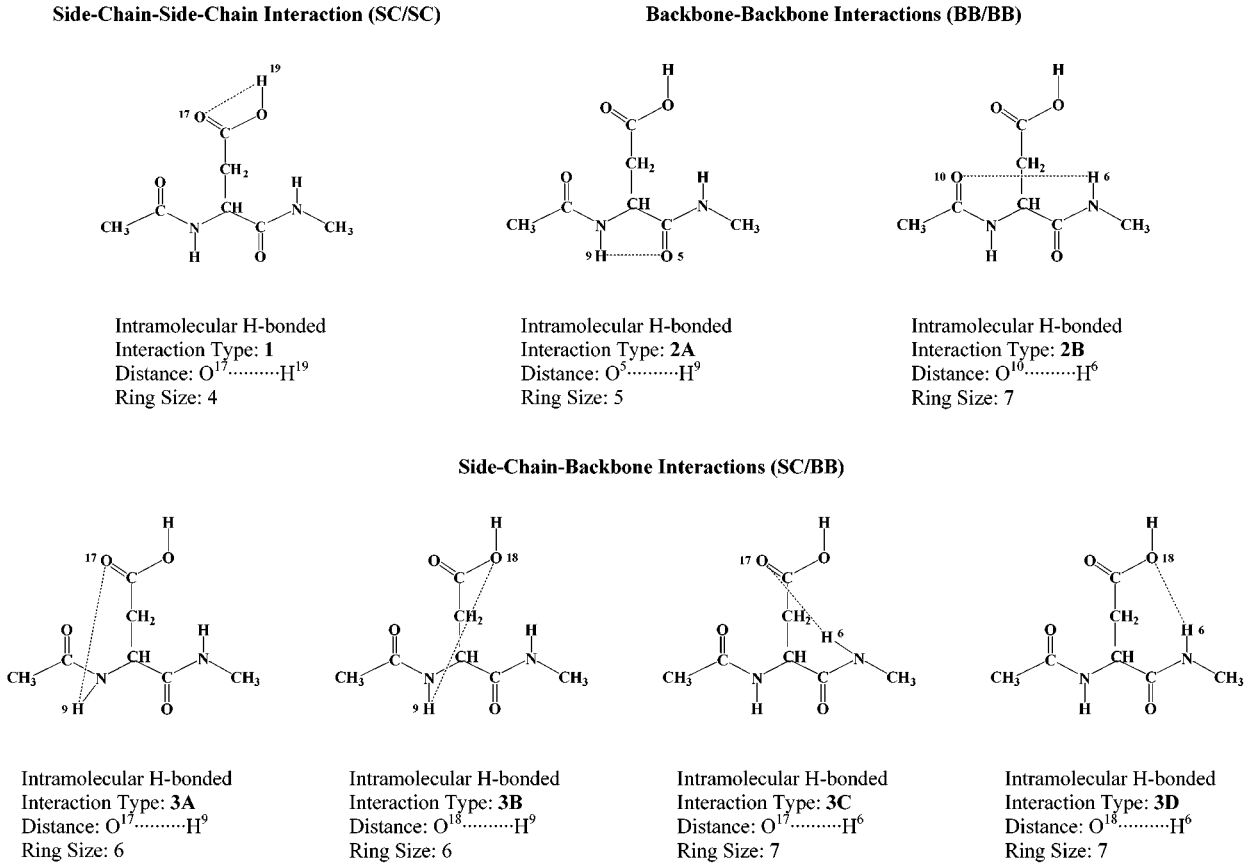

Figure 8. Classification of the types of internal hydrogen bonding for *N*-acetyl-L-aspartic acid *N*′-methylamide.

interaction that existed in all stable conformers found for the aspartic acid residue. Since all stable conformers possess this SC/SC interaction, it is plausible that this type of hydrogen bonding serves to stabilize the general structure of the amino acid in the *endo* orientation. In addition to the SC/SC interaction, there exist two backbone−backbone (BB/BB) interactions and four side-chain-backbone (SC/BB) interactions. The BB/BB interaction can be viewed as an internal stabilizing factor that allows fundamental stability for the aspartic acid residue while at the same time allowing the side chain to participate in external interactions with other substrates. On the other hand, the SC/BB interaction can induce even greater internal stability to the aspartic acid residue than the SC/SC interaction. An example to illustrate this phenomenon exists in the g^-s^- of the α_L conformation. Here, type 3A of the hydrogen bond interaction seems to contribute a major stabilizing force that allows for the existence of this unlikely found conformer at the α_L backbone. Moreover, it is worth noting that a rather weak H···N interaction (distance = 2.2758, not included in Table 3) seems to exist for the α_L conformer, shown in Figure 9. Such unusual interaction, which could be categorized as a BB/BB interaction (although not shown in Figure 8), may also be a contributing reason of the existence of the α_L conformer. A correlating trend between hydrogen bond distance and ring size (RS) is shown in Figure 10. Here, it is apparent that the shorter the hydrogen bond distance, the greater the RS. The overall correlation equation shows a least-squares value of $R^2 = 0.8443$, showing that such trend is rational and realistic.

In Figure 11, various stabilization energies, with respect to either β_L or γ_L of the glycine residue, are shown in a bar-graph format. The difference in stabilization energy, ΔE^{stabil} with respect to β_L and with respect to γ_L is constant (1.13 kcal/mol), as shown in Figure 5. Consequently, it is enough to discuss

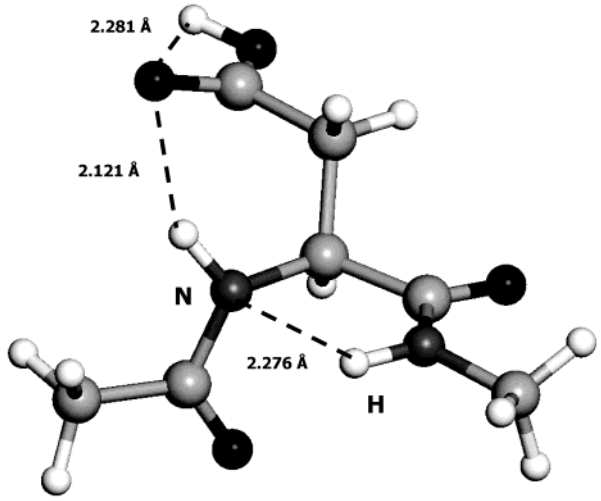

Figure 9. A new type of backbone−backbone (−CON−H···NHCO−) hydrogen bonding observed in the case of the α_L [g^-s^-] conformation at H···N distance of 2.276 Å in addition to regular hydrogen bonds.

only one set of the stabilization energy data. Here, we chose to discuss the values with respect to the β_L glycine residue showing at the right-hand side of Figure 11. One can observe that the L-substituted conformation (i.e., γ_L, β_L, δ_L, α_L) of the aspartic acid residue is more stable than its D-substituted form (i.e., γ_D, ϵ_D, δ_D, α_D). As illustrated in Figure 11, most of the L conformers are stabilized. This is shown by the fact that the L-subscripted stable conformers for *N*-acetyl-L-aspartic acid *N*′-methylamide either have great negative values or small positive values for their stabilization energies. This trend is observed in the γ_L, β_L δ_L, and α_L backbones for the aspartic acid residue. On the other hand, most conformers found for the D-subscripted

TABLE 3: The Relative Distances of Potential Hydrogen Bonds of *N*-Acetyl-L-aspartic acid *N*′-Methylamide in Its *endo* Form for All Its Stable Backbone (γ_L, β_L, δ_L, α_L, γ_D, δ_D, α_D, and ϵ_D) Conformations Computed at the B3LYP/6-31G(d) Level of Theory[a]

final conformation	interaction type			distance (Å)						
BB [$\chi_1\chi_2$]	SC/SC	BB/BB	SC/BB	O17−H19	H9−17	H9−18	H9−5	H6−−10	H6−17	H6−018
				γ_L Backbone Conformation						
γ_L [g^+s^+]	1	2B	3A	2.274	2.056	3.924	3.565	2.030	4.945	5.833
γ_L [g^+g^-]	1	2B	3B	2.276	4.026	2.109	3.554	2.053	5.858	4.893
γ_L [as]	1	2B		2.282	4.911	4.701	3.632	2.044	5.761	4.260
γ_L [aa]	1	2B		2.283	4.774	4.895	3.588	2.066	4.277	5.797
γ_L [g^-s^+]	1	2B		2.281	3.778	2.419	3.747	1.986	5.506	5.566
γ_L [g^-a]	1	2B		2.280	3.638	3.859	3.720	2.004	4.922	6.155
γ_L [g^-s^-]	1	2B	3A	2.275	2.097	3.807	3.834	1.952	5.416	5.873
				β_L Backbone Conformation						
β_L [g^+s^+]	1	2A		2.281	2.906	4.064	2.261	4.891	5.233	4.343
β_L [g^+a][b,c]	1	2A		2.282	3.161	4.713	2.117	5.099	3.719	4.322
β_L [ag^+]	1	2A	3D	2.266	5.406	4.935	2.120	4.999	3.587	2.196
β_L [aa]	1	2A	3C	2.270	4.988	5.509	2.074	5.040	1.984	3.864
				δ_L Backbone Conformation						
δ_L [g^+a][b,c]	1		3A	2.275	2.179	4.031	3.850	3.588	4.038	5.649
δ_L [g^+s]	1		3B	2.270	4.129	2.215	3.832	3.543	5.674	4.065
δ_L [ag^+]	1			2.282	5.107	4.838	3.784	3.617	5.887	4.899
δ_L [g^-g^+]	1			2.271	4.514	3.111	3.921	3.649	5.828	5.281
δ_L [g^-s^-]	1			2.286	2.950	4.333	3.978	3.641	5.245	5.773
				α_L Backbone Conformation						
α_L [g^-s^-][b,c]	1		3A	2.281	2.121	3.843	4.397	3.014	4.822	5.831
				γ_D Backbone Conformation						
γ_D [ag^+]	1	2B		2.288	5.505	4.611	3.941	1.927	4.230	4.972
γ_D [as^-][b,c]	1	2B		2.282	4.558	5.581	3.754	1.957	4.856	4.483
γ_D [g^-a]	1	2B		2.282	2.787	4.517	4.096	1.873	4.856	5.279
γ_D [g^-g^-]	1	2B		2.271	4.307	3.193	3.992	1.894	4.856	5.111
				δ_D Backbone Conformation						
δ_D [g^+g^+][b,c]	1		3D	2.250	4.467	3.351	3.623	4.853	4.126	2.078
δ_D [g^+a][b,c]	1		3C	2.265	3.075	4.664	3.624	4.874	1.961	3.961
δ_D [g^+g^-]	1		3D	2.247	4.876	3.084	3.608	4.760	3.630	2.151
δ_D [ag^+]	1			2.288	5.341	5.097	3.554	4.602	4.205	4.952
δ_D [as^-]	1			2.282	5.154	5.363	3.573	4.532	5.105	4.349
δ_D [g^-g^-][b,c]	1			2.303	4.032	4.740	3.570	5.004	4.531	5.101
				α_D Backbone Conformation						
α_D [g^+s^+]	1			2.283	3.329	4.602	4.456	2.800	5.109	5.092
α_D [g^+g^-]	1			2.268	4.793	3.475	4.453	2.713	5.081	4.996
α_D [ag^+]	1			2.274	5.453	4.439	4.428	3.070	5.888	4.999
α_D [as^-]	1			2.278	4.445	5.421	4.424	3.143	5.063	5.913
α_D [g^-a]	1			2.275	2.528	4.295	4.437	2.993	5.048	6.198
α_D [g^-s]	1			2.261	4.199	2.721	4.438	2.974	6.132	5.031
				ϵ_D Backbone Conformation						
ϵ_D [g^+g^+]	1		3D	2.293	4.062	4.881	3.321	2.932	3.782	2.030
ϵ_D [g^+s^-]	1		3C	2.279	5.051	4.461	2.990	3.281	1.942	3.740
ϵ_D [s^-a]	1		3C	2.268	4.856	5.512	2.783	4.718	1.966	3.800
ϵ_D [s^-g^-]	1		3D	2.273	5.203	4.879	2.763	4.444	3.960	2.025

[a] No conformers were found for the ϵ_L backbone, and hence, no hydrogen bond distances for the ϵ_L backbone could be tabulated. [b] After 200 iterations under B3LYP/6-31G(d) at (TIGHT, Z-MATRIX), the force has converged, but the displacement did not converge completely. [c] This result was obtained from an optimization fully converged under regular B3LYP/6-31G(d) at (Z-MATRIX).

form of the aspartic acid residue are in general de-stabilized. Again, shown in Figure 11, the D-subscripted conformers have either great positive values or small negative values for their stabilization energies. This trend exists in the α_D, γ_D, δ_D, and ϵ_D backbones for the aspartic acid residue. An analogous trend is also shown in the stabilization energy values calculated with respect to γ_L, at the left-hand side of Figure 11.

Interestingly, we also observed that in some cases, the ω_0 torsional angle of some stable conformers (such as those found in the α_D conformation) have deviated from the ideal value of 180°. Such an example can be found at the δ_L [g^-s^-], α_L [g^-s^-], α_D [g^+s^+], and ϵ_D [s^-a] conformers. One possible reason for such rather strange occurrences may due to the existence of hydrogen bond interactions that act as stabilizing forces for these conformers. For instance, the δ_L [g^-s^-] conformer has a potential hydrogen bond interaction (2.950 Å) between H^{19} and O^{17}, as shown in Table 3. Although this particular interaction, a potential SC/BB, was not categorized as a hydrogen bond (our definition for a hydrogen bond interaction of *N*-acetyl-L-aspartic acid *N*′-methylamide in its *endo* form is 2.300 Å), it

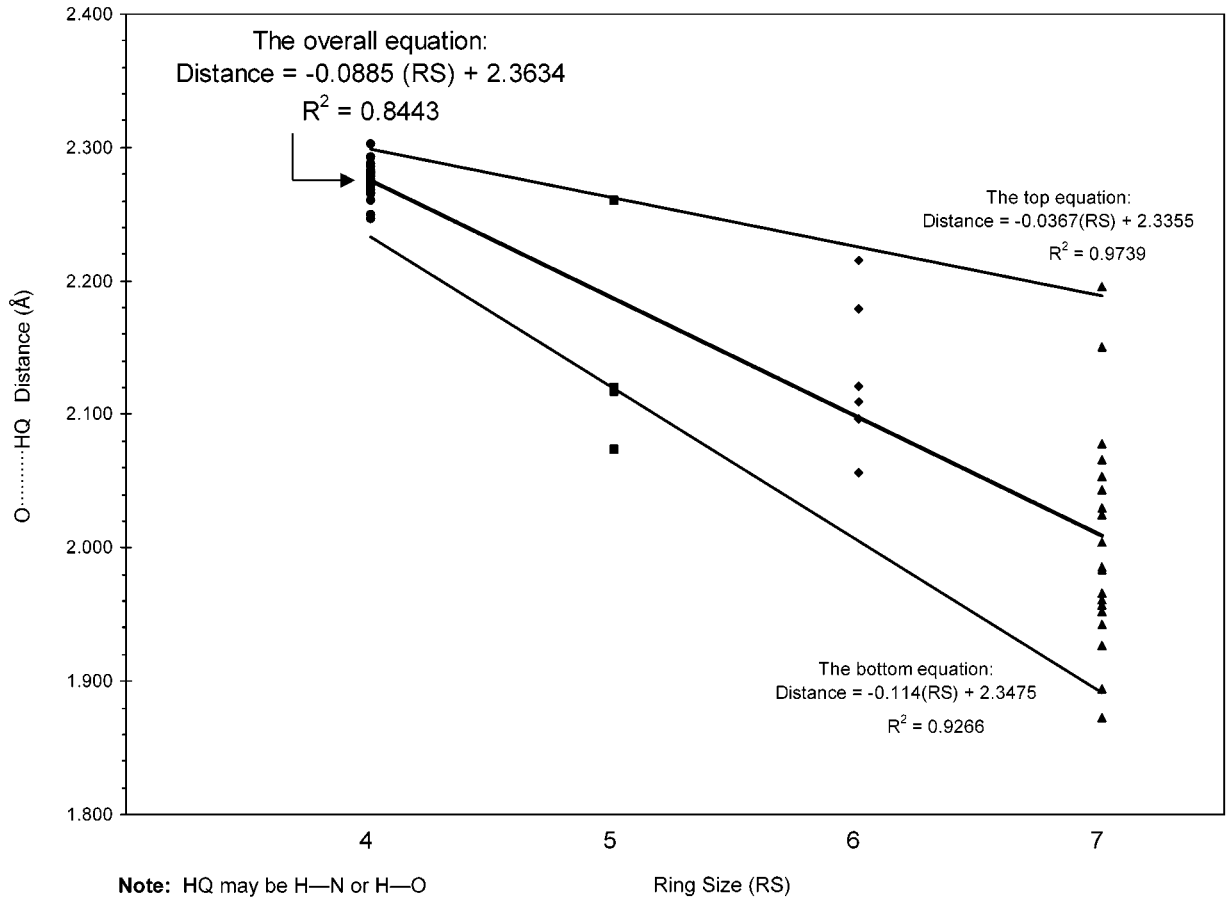

Figure 10. A trend showing the interrelation between hydrogen-bonded distance and ring size (RS) of internal hydrogen bonds of *N*-acetyl-L-aspartic acid *N*′-methylamide.

shows that it has a slight inclination in forming a potential interaction that can act as a stabilizing factor for the conformer. Likewise, other conformers mentioned above which have deviated ω_0 angles all have at least one other type of potential hydrogen bonding that can act as important stabilizing forces for the conformer itself. In addition, this may suggest that as a particular conformer seeks to stabilize its side-chain with its backbone, it may be willing to rotate one of its adjacent peptide bonds away from coplanarity. This mechanism is one of compromise, where a conformer may change, for example, its ω_0 torsional angle in order to form a weak hydrogen bond that may stabilize itself even to a greater extent. Such an observation may deem important when considering the aspartic acid residue's role in the RGD tripeptide. If it is true that the aspartic acid is willing to offset its torsional angles in order to achieve greater stability, then it can also do in concordance with other members of the RGD moiety, namely, arginine and glycine, for an overall stability of the tripeptide. In this case, it is very likely that significant BB/BB and SC/BB interactions would be involved in the overall stability of the RGD. Hence, it is not surprising to recognize from Table 3 that aside from the SC/SC interaction there are two additional hydrogen bond types, namely, BB/BB and SC/BB, that help to stabilize the conformers of the γ_L and β_L backbones. Interestingly, these two backbones are traditionally known as being the more stabilized conformations, where most of the stable conformers of an amino acid would most likely be found. Both BB/BB and SC/BB interactions allow the aspartic acid residue to achieve internal stabilization while acting as stabilizing forces for the other members of the RGD. The study of SC/BB and BB/BB interactions in *N*-acetyl-L-aspartic acid *N*′-methylamide may deem significant as these interactions may present not only in the internal stabilization within the RGD but also in the external stability of the tripeptide during its binding to a foreign substrate. Since substrate binding is greatly affected by the 3D steric arrangement of molecules, it is then logical to study the stabilizing interactions within the molecules themselves. In turn, this will allow for more in-depth understanding of what brings about the different conformations for a particular substrate-binding assay.

Conclusions

The conformational preferences for the *endo* form of *N*-acetyl-L-aspartic acid-*N*′-methylamide were determined by quantum chemical calculations at the B3LYP/6-31G(d) *ab initio* level. We found and optimized a total of 37 stable conformers (out of the possible 81) for the aspartic acid residue at this level of theory. All relative energies, including the stabilization exerted by the sidechain on the backbone, have been calculated for the 37 stable conformers.

For this particular aspartic acid residue, various BB/BB (N−H···O═C) and BB/SC (N−H···O═C; N−H···OH) hydrogen bonds were analyzed. There exists a SC/SC interaction in all 37 stable conformers, indicating that this interaction is important for the general stabilization of the *endo* form of the aspartic acid residue. In addition, we observed two BB/BB interactions and four SC/BB interactions among the stable conformers. The internal hydrogen bonding may deem significant if the aspartyl residue were to participate in intra- or intermolecular interactions in polypeptides, such as in the RGD tripeptide. This is because these internal stabilizing forces may be disrupted to allow for the folding or unfolding of the overall polypeptide into a particular geometry.

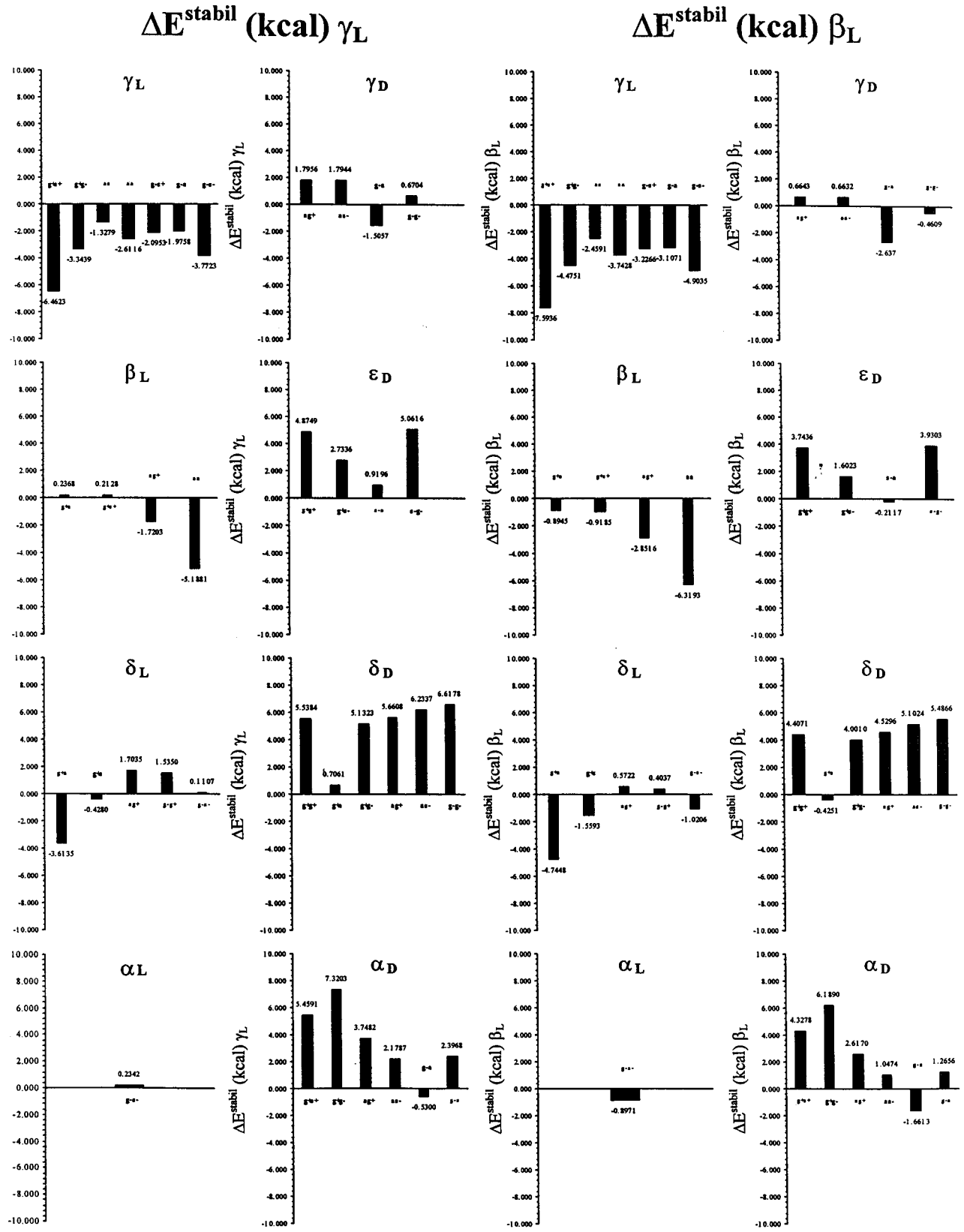

Figure 11. Computed stabilization energies of *N*-acetyl-L-aspartic acid *N*′-methylamide with respect to γ_L and β_L backbone conformation of *N*-acetyl-L-aspartic acid *N*′-methylamide.

In this work, the stable g^-s^- conformer found at the α_L backbone may represent a novel geometry in which the aspartyl residue may arrange itself during such peptide folding.

Acknowledgment. The authors express their gratitude for the generous allocation of CPU time provide by the National Cancer Institute (NCI) at the Frederick Biomedical Supercomputing Center.

References and Notes

(1) Perczel, A.; Csizmadia, I. G. *Int. Rev. Phys. Chem.* **1995**, *14*, 127.

(2) Chasse, G. A.; Rodriguez, A. M.; Mak, M. L.; Deretey, E.; Perczel, A.; Sosa, C. P.; Enriz, R.D.; Csizmadia, I. G. *J. Mol. Struct (THEOCHEM)* **2001**, *537*, 319.

(3) McAllister, M. A.; Endrédi, G.; Viviani, W.; Perczel, A.; Császár, P.; Ladik, J.; Rivail, J.-L.; Csizmadia, I. G. *Can. J. Chem*. **1995**, *73*, 1563.

(4) Liegener, C.-M.; Endrédi, G.; McAllister, M. A.; Perczel, A.; Ladik, J.; Csizmadia, I. G. *J. Am. Chem. Soc*. **1993**, *115*, 8275.

(5) Endrédi, G.; Liegner, C.-M.; McAllister, M. A.; Perczel, A.; Ladik, J.; Csizmadia, I. G. *J. Mol. Struct (THEOCHEM)* **1994**, *306*, 1.

(6) Endrédi, G.; McAllister, M. A.; Perczel, A.; Császár, P.; Ladik, J.; Csizmadia, I. G. *J. Mol. Struct (THEOCHEM)* **1995**, *331*, 5.

(7) Endrédi, G.; McAllister, M. A.; Farkas, Ö.; Perczel, A.; Ladik, J.; Csizmadia, I. G. *J. Mol. Struct (THEOCHEM)* **1995**, *331*, 11.

(8) Berg, M.; Salpietro, S. J.; Perczel, A.; Farkas, Ö.; Csizmadia, I. G. *J. Mol. Struct. (THEOCHEM)* **2000**, *504*, 127.

(9) Perczel, A.; Farkas, Ö.; Csizmadia, I. G. *J. Am. Chem. Soc*. **1995**, *117*, 1653.

(10) Baldoni, H. A.; Zamarbide, G. N.; Enriz, R. D.; Jauregui, E. A.; Farkas, Ö.; Perczel, A.; Salpietro, S. J.; Csizmadia, I. G. *J. Mol. Struct.* **2000**, *500* (Millennium Volume), 97.

(11) Viviani, W.; Rivail, J.-L.; Perczel, A.; Csizmadia, I. G. *J. Am. Chem. Soc*. **1993**, *115*, 8321.

(12) Farkas, Ö.; McAllister, M. A.; Ma, J. H.; Perczel, A.; Hollósi, M.; Csizmadia, I. G. *J. Mol. Struct (THEOCHEM)* **1996**, *369*, 105.

(13) Perczel, A.; Farkas, Ö.; Csizmadia, I. G. *Can. J. Chem*. **1997**, *75*, 1120.

(14) Jakli, I.; Perczel, A.; Farkas, Ö.; Hollosi, M.; Csizmadia, I. G. *J. Mol. Struct (THEOCHEM)* **1998**, *455*, 303.

(15) Perczel, A.; Farkas, Ö.; Csizmadia, I. G. *J. Comput. Chem*. **1996**, *17*, 821.

(16) Perczel, A.; Farkas, Ö.; Csizmadia, I. G. *J. Am. Chem. Soc*. **1996**, *118*, 7809.

(17) Jakli, I.; Perczel, A.; Farkas, Ö.; Sosa, C. P.; Csizmadia, I. G. *J. Comput. Chem*. **2000**, *21*, 626.

(18) Tarditi, M.; Klipfel, M. W.; Rodriguez, A. M.; Suvire, F. D.; Chasse, G. A.; Farkas, O.; Perczel, A.; Enriz, R. D. *J. Mol. Struct. (THEOCHEM)* **2001**, *545*, 29.

(19) Masman, M. F.; Amaya, M. G.; Rodriguez, A. M.; Suvire, F. D.; Chasse, G. A.; Farkas, O.; Perczel, A.; Enriz, R. D. *J. Mol. Struct. (THEOCHEM)* **2001**, *543*, 203.

(20) Barroso, M. N.; Cerutti, E. S.; Rodriguez, A. M.; Jauregui, E. A.; Farkas, O.; Perczel, A.; Enriz, R. D. *J. Mol. Struct. (THEOCHEM)* **2001**, *548*, 21.

(21) Zamora, M. A.; Baldoni, H. A.; Bombasaro, J. A.; Mak, M. L.; Perczel, A.; Farkas, O.; Enriz, R. D. *J. Mol. Struct. (THEOCHEM)* **2001**, *540*, 271.

(22) Vank, J. C.; Sosa, C. P.; Perczel, A.; Csizmadia, I. G. *Can. J. Chem*. **2000**, *78*, 395.

(23) Baldoni, H. A.; Rodriguez, A. M.; Zamarbide, G.; Enriz, R. D.; Farkas, Ö.; Csaszar, P.; Torday, L. L.; Sosa, C. P.; Jakli, I.; Perczel, A.; Hollosi, M.; Csizmadia, I. G. *J. Mol. Struct. (THEOCHEM)* **1999**, *465*, 79.

(24) Salpietro, S. J.; Perczel, A.; Farkas, Ö.; Enriz, R. D.; Csizmadia, I. G. *J. Mol. Struct. (THEOCHEM)* **2000**, *497*, 39.

(25) Percel, A.; Ángyán, J. G.; Kajtár, M.; Viviani, W.; Rivail, J. L.; Marcoccia, J. F.; Csizmadia, I. G. *J. Am. Chem. Soc*. **1991**, *113*, 6256.

(26) McAllister, M. A.; Perczel, A.; Császár, P.; Viviani, W.; Rivail, J. L.; Csizmadia, I. G. *J. Mol. Struct. (THEOCHEM)* **1993**, *288*, 161.

(27) McAllister, M. A.; Perczel, A.; Császár, P.; Csizmadia, I. G. *J. Mol. Struct. (THEOCHEM)* **1993**, *288*, 181.

(28) Perczel, A.; McAllister, M. A.; Császár, P.; Csizmadia, I. G. *Can. J. Chem*. **1994**, *72*, 2050.

(29) Cheung, M.; McGovern, M. E.; Jin, T.; Zhao, D. C.; McAllister, M. A.; Perczel, A.; Császár, P.; Csizmadia, I. G. *J. Mol. Struct. (THEOCHEM)* **1994**, *309*, 151.

(30) Rodriguez, A. M.; Baldoni, H. A.; Suvire, F.; Nieto-Vasquez, R.; Zamarbide, G.; Enriz, R. D.; Farkas, Ö.; Perczel, A.; Csizmadia, I. G. *J. Mol. Struct. (THEOCHEM)* **1998**, *455*, 275.

(31) Berg, M. A.; Chasse, G. A.; Deretey, E.; Füzéry, A. K.; Fung, B. M.; Fung, D. Y. K.; Henry-Riyad, H.; Lin, A. C.; Mak, M. L.; Mantas, A.; Patel, M.; Repyakh, I. V.; Staikova, M.; Salpietro, S. J.; Tang, T.-H.; Vank, J. C.; Perczel, A.; Farkas, Ö.; Torday, L. L., Székely, Z.; Csizmadia, I. G. *J. Mol. Struct. (THEOCHEM)* **2000**, *500*, 5.

(32) Horster, A.; Teichmann, B.; Hormes, R.; Grimm, D.; Kleinschmidt, J.; Sczakiel, G. *Gene Ther*. **1998**, *6*, 1231.

(33) Inouye, R. T.; Du, B.; Boldt-Houle, D.; Ferrante, A.; Park, I. W.; Hammer, S. M.; Duan, L.; Groopman, J. E.; Pomerantz, R. J.; Terwilliger, E. F. *J. Virol*. **1997**, *71*, 4071.

(34) Magnusson, M. K.; Hong, S. S.; Boulanger, P.; Lindholm, L. *J. Virol*. **2001**, *75*, 7280.

(35) Okada, N.; Tsukada, Y.; Nakagawa, S.; Mizuguchi, H.; Mori, K.; Saito, T.; Fujita, T.; Yamamoto, A.; Hayakawa, T.; Mayumi, T. *Biochem. Biophys. Res. Commun*. **2001**, *282*, 173.

(36) Hay, C.; De Leon, H.; Jafari, J. D.; Jakubczak, J. L.; Mech, C. A.; Hallenbeck, P. L.; Powell, S. K.; Liau, G.; Stevenson, S. C. *J. Vasc. Res*. **2001**, *38*, 315.

(37) Hatse, S.; Princen, K.; Gerlach, L. O.; Bridger, G.; Henson, G.; De Clercq, E.; Schwartz, T. W.; Schols, D. *Mol. Pharmacol*. **2001**, *60*, 164.

(38) Anuradha, C. D.; Kanno, S.; Hirano, S. *Cell Biol. Toxicol*. **2000**, *16*, 275.

(39) Kuroda, K.; Miyata, K.; Fujita, F.; Koike, M.; Fujita, M.; Nomura, M.; Nakagawa, S.; Tsutsumi, Y.; Kawagoe, T.; Mitsuishi, Y.; Mayumi, T. *Cancer Lett*. **2000**, *159*, 33.

(40) Demougeot, C.; Garnier, P.; Mossiat, C.; Bertrand, N.; Giroud, M.; Beley, A.; Marie, C. *J. Neurochem*. **2001**, 77, 408.

(41) Collins, M. J.; Waite, E. R.; van Duin, A. C. *Philos. Trans. R. Soc. London, Ser. B. Biol. Sci*. **1999**, *354*, 51.

(42) Heine, A.; Stura, E. A.; Yli-Kauhaluoma, J. T.; Gao, C.; Deng, Q.; Beno, B. R.; Houk, K. N.; Janda, K. D.; Wilson, I. A. *Science*. **1998**, 279, 1934.

(43) Hoffmann, R.; Craik, D. J.; Bokonyi, K.; Varga, I.; Otvos, L., Jr. *J. Pept. Sci*. **1999**, *5*, 442.

(44) Contreras, J. A.; Karlsson, M.; Østerlund, T.; Laurell, H.; Svensson, A.; Holm, C. *J. Biol. Chem*. **1996**, *271*, 31426.

(45) Short, G. F. 3rd; Laikhter A. L.; Lodder, M.; Shayo, Y.; Arslan, T.; Hecht, S. M. *Biochemistry*. **2000**, *39*, 8768.

(46) Hu, R.; Bekisz, J.; Schmeisser, H.; McPhie, P.; Zoon, K. *J. Immunol*. **2001**, *167*, 1482.

(47) Saadat, D.; Harrison, D. H. *Biochemistry*. **1998**, *37*, 10074.

(48) Ghandehari, H,; Sharan, R.; Rubas, W.; Killing, W. M. *J. Pharm. Pharm. Sci*. **2001**, *4*, 32.

(49) Frisch, M. J.; Trucks, G. W.; Schlegel, H. B.; Gill, P. M. W.; Johnson, B. G.; Robb, M. A.; Cheeseman, J. R.; Keith, T.; Petersson, G. A.; Montgomery, J. A.; Raghavachari, K.; Al-Laham, M. A.; Zakrzewski, V. G.; Ortiz, J. V.; Foresman, J. B.; Cioslowski, J.; Stefanov, B. B.; Nanayakkara, A.; Challacombe, M.; Peng, C. Y.; Ayala, P. Y.; Chen, W.; Wong, M. W.; Andres, J. L.; Replogle, E. S.; Gomperts, R.; Martin, R. L.; Fox, D. J.; Binkley, J. S.; Defrees, D. J.; Baker, J.; Stewart, J. P.; Head-Gordon, M.; Gonzalez, C.; Pople, J. A. *Gaussian 94*; Gaussian, Inc.: Pittsburgh, PA, 1995.

(50) Frisch, M. J.; Trucks, G. W.; Schlegel, H. B.; Scuseria, G. E.; Robb, M. A.; Cheeseman, J. R.; Zakrzewski, V. G.; Montgomery, J. A., Jr.; Stratmann, R. E.; Burant, J. C.; Dapprich, S.; Millam, J. M.; Daniels, A. D.; Kudin, K. N.; Strain, M. C.; Farkas, O.; Tomasi, J.; Barone, V.; Cossi, M.; Cammi, R.; Mennucci, B.; Pomelli, C.; Adamo, C.; Clifford, S.; Ochterski, J.; Petersson, G. A.; Ayala, P. Y.; Cui, Q.; Morokuma, K.; Malick, D. K.; Rabuck, A. D.; Raghavachari, K.; Foresman, J. B.; Cioslowski, J.; Ortiz, J. V.; Stefanov, B. B.; Liu, G.; Liashenko, A.; Piskorz, P.; Komaromi, I.; Gomperts, R.; Martin, R. L.; Fox, D. J.; Keith, T.; Al-Laham, M. A.; Peng, C. Y.; Nanayakkara, A.; Gonzalez, C.; Challacombe, M.; Gill, P. M. W.; Johnson, B. G.; Chen, W.; Wong, M. W.; Andres, J. L.; Head-Gordon, M.; Replogle, E. S.; Pople, J. A. *Gaussian 98*; Gaussian, Inc.: Pittsburgh, PA, 1998.